American Journal of Psychiatric Rehabilitation

Expert Opinion Article

Automated Brain Tumor Detection And Localization Using YOLO-Based Deep Learning Algorithm

Satheesh Kumar K[1]*, Ahmed Riyas Kaan A[2], Hariharan P[3], Surya N[4]

[1]*Department of Computer Science and Engineering, University College of Engineering, Thirukkuvalai (A Constituent College of Anna University, Chennai) Nagapattinam, India, sat1984mca@gmail.com
[2]Department of Computer Science and Engineering, University College of Engineering, Thirukkuvalai (A Constituent College of Anna University, Chennai) Nagapattinam, India, Riyaskaan387@gmail.com
[3]Department of Computer Science and Engineering, University College of Engineering, Thirukkuvalai (A Constituent College of Anna University, Chennai) Nagapattinam, India, hariharan15022003@gmail.com
[4]Department of Computer Science and Engineering, University College of Engineering, Thirukkuvalai (A Constituent College of Anna University, Chennai) Nagapattinam, India, suryakash2004@gmail.com

Abstract
Classifying brain diseases is a very difficult task because of their complexity and sensitivity. Developing an efficient treatment plan calls for early detection and diagnosis since brain tumors are severe and occasionally fatal. A key medical imaging tool, magnetic resonance imaging (MRI) enables the thorough, non-invasive view of the internal structures of the brain. Magnetic resonance imaging (MRI) is essential for diagnosing and treating brain tumors. Beginning with dataset preprocessing, the approach is applicable to MRI scans and clinical data from individuals with various brain disorders, including tumor and non-tumor cases. The dataset consists of training and testing sets. Detecting MRI tumors calls for several procedures including feature extraction, classification, and image post-processing. The system uses the YOLO (You Only Look Once) algorithm with the CNN model, a pre-trained model using the concept of transfer learning, for classifying and detecting brain tumors. The proposed framework not only improves the performance of training a better model by using the pre-trained model but also refines the dataset for better accuracy by using thresholding and increases the number of images in the dataset by using data augmentation. Early results indicate that the family of YOLO models outperforms earlier architectures since it uses a compound coefficient with a constant ratio to scale all depth, width, and resolution of an image. The findings also showed that by increasing the baseline architecture, the model can capture complex features, and thus the overall performance of the system is significantly improved.

Keywords: Brain tumor detection, deep learning, image processing, MRI, YOLOv11

I. INTRODUCTION

The brain, one of the most important organs in the human body, controls the function of every other organ and helps with decision-making. It acts as the command center for the central nervous system and is primarily responsible for controlling the daily voluntary and involuntary bodily functions. Inside our brain, a tumor is an unchecked, growing mass of unwanted tissue that resembles a fibrous web. This year, about 3,540 children under the age of 15 receive a brain tumor diagnosis. To prevent and treat the condition, it is essential to have a thorough understanding of brain tumors and their stages.

An abnormal mass of tissue where cells proliferate and grow out of control, apparently unaffected by the systems that regulate healthy cells, is known as an intracranial tumor, or brain tumor. Primary and metastatic brain tumors are the two main types of brain tumors, though there are over 150 different types known to exist. Primary brain tumors are those that originate in the tissues of the brain or the tissues that surround the brain. Glial (composed of glial cells) or non-glial (developed on or in the brain's structures, such as nerves, blood vessels, and glands) primary tumors can be either benign or malignant. Metastatic brain tumors are those that start in other parts of the body, such as the breast or lungs, and travel to the brain, typically through the bloodstream. Metastatic tumors are classified as cancer because they are malignant.

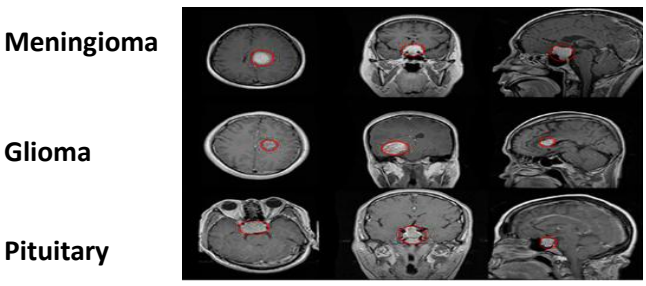

II. LITERATURE REVIEW

Deep learning has gained popularity for brain tumor detection because of its high accuracy and speed in processing MRI images. Using publicly accessible MRI datasets, researchers have put forth a number of strategies to increase the effectiveness of classification and detection.

VGG19 and ResNext101_32×8d models, improved by hyperparameter tuning and transfer learning, were employed by Aeed Mohsen et al. [1]. They used a six-step process that included training, performance evaluation, and image preprocessing. With 94.5% and 92.8% accuracy, respectively, the models demonstrated efficacy in tumor classification at a low computational cost.

The difficulties caused by MRI artifacts and Rician noise, which impair the precision of medical image classification, were brought to light by Solanki et al. [2]. For greater robustness across a range of images, they recommended combining handcrafted features with deep features and underlined the necessity for generalized approaches.

In order to increase diagnostic accuracy, Shah et al. [3] presented VS-BEAM, an ensemble-based CNN architecture with Squeeze-and-Excitation (SE) blocks, which uses a voting mechanism. Their model handled multiclass classification problems well, outperforming standalone CNNs with an accuracy of 96.12%.

The LCDEiT framework was proposed by Ferdous et al. [4], who combined a transformer-based student model with external attention with a CNN-based teacher. It demonstrated high accuracy with efficient computation, achieving F1-scores of 0.978 and 0.937 when tested on the Figshare and BraTS-21 datasets.

In an IoMT setup, Ramprasad et al. [5] combined RU-Net, BWO-GA, and AlexNet for classification and privacy protection. Their system safely transmitted medical images with an accuracy of 95.6%.

In contrast to these techniques, our system uses YOLOv11 to locate and identify brain tumors in real time.

III. IMPLEMENTATION

A. *Dataset*

The MRI dataset used by the brain tumor detection system was personally collected from a range of medical imaging sources, such as T1-weighted brain scans with contrast enhancement. The dataset is separated into four carefully selected categories: pituitary, glioma, meningioma, and no tumor. Each class contains a balanced number of labeled images to enable effective training and testing of the YOLOv11 model. These MRI scans were gathered in collaboration with local scan facilities and verified by medical professionals to ensure superior and accurate representation. Images were manually labeled with bounding boxes to indicate tumor regions in order to produce a reliable dataset for object detection tasks. The dataset was divided into training, validation, and testing sets to guarantee robustness, which improved generalization and reduced overfitting. The system's dependability and relevance in the real world are enhanced by this specially gathered dataset.

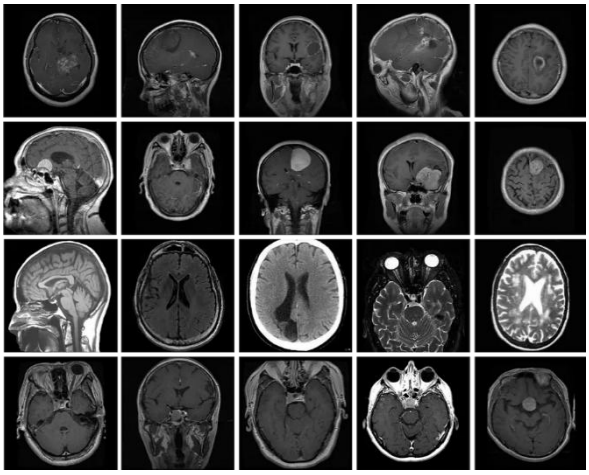

Figure 2: *Dataset Sample*

B. *Preprocessing*

i) Image Resizing: All MRI images are resized to 416×416 pixels in order to meet the YOLOv11 input dimensions. This standardization reduces the computational load and ensures consistent performance during detection.

ii) Noise Filtering: MRI images often contain noise due to imaging artifacts. A Gaussian blur is used to smooth the image and remove high-frequency noise, making important features like tumor boundaries more visible. This improves the model's ability to extract relevant features and lowers false detections.

Pixel values are also normalized to standard ranges and converted to grayscale when necessary to reduce color redundancy. These preprocessing techniques help the model focus on important regions, which improves detection accuracy and reliability in clinical applications.

C. *Prediction*

The MRI images are preprocessed and then run through the trained YOLOv11 model, which carries out two crucial functions: classification and localization. The model simultaneously assigns a tumor type based on learned features while scanning the image and drawing bounding boxes around abnormal regions (tumors) that are detected. The prediction output comprises the coordinates of the t_x, t_y, t_w, t_h, and t_0

These stand for the width (w), height (h), bounding box center coordinates (x,y), width (w), and objectness score (t_0). The following transformation equations are used to determine the final bounding box coordinates:

$$b_x=\sigma(t_x)+c_x \qquad b_y=\sigma(t_y)+c_y$$

$$b_w=p_w \cdot e^{t_w} \qquad b_h=p_h \cdot e^{t_h}$$

Where:

- (c_x, c_y) is the top-left corner of the grid cell,
- p_w, p_h are anchor box dimensions,
- σ is the sigmoid function to constrain t_x, t_y between 0 and 1.

The final confidence score is:

Confidence = $\sigma(t_0)$ ⍰ IoU (pred, truth)

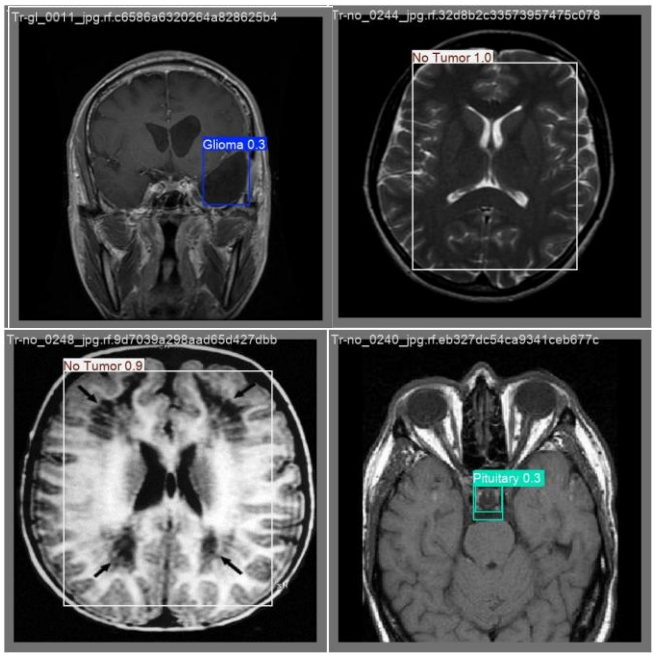

Figure 3: *Bounding Box*

IV. RESULT

After 20 implementation epochs, the performance of the suggested model is assessed using parameters extracted from the Confusion Matrix. The ability of the proposed model to classify input images from the

dataset into four different types of brain tumors is used to evaluate its performance.

A. *Accuracy Analysis*

The precision and accuracy of the model's predictions are assessed by the Precision-Confidence Curve (figure 4).

The model achieved 100% precision at a strict 99.2% confidence threshold, meaning that there were no false positives.

Meningioma demonstrated its strong detectability by maintaining high precision across the majority of thresholds.

Despite starting at a lower base than other classes, Glioma demonstrated an increase in precision as confidence.

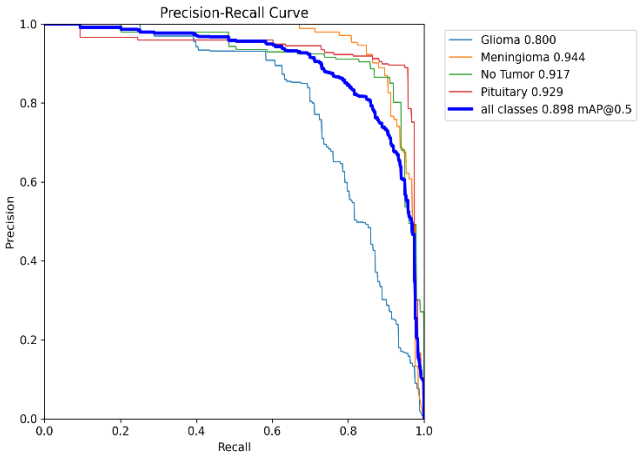

Figure 4: *Accuracy Analysing Graph*

B. *Confusion Matrix*

The model's ability to differentiate between five classes—glioma, meningioma, no tumor, pituitary, and background—is demonstrated by the confusion matrix (Figure 5).

With a classification accuracy of more than 85%, glioma and meningioma were accurately predicted.

In more than 88% of the cases, pituitary tumors were accurately identified.

There were a few minor misclassifications, mostly between Background and No Tumor, which marginally reduced the accuracy of those classes.

All categories combined have an overall classification accuracy of about 86%.

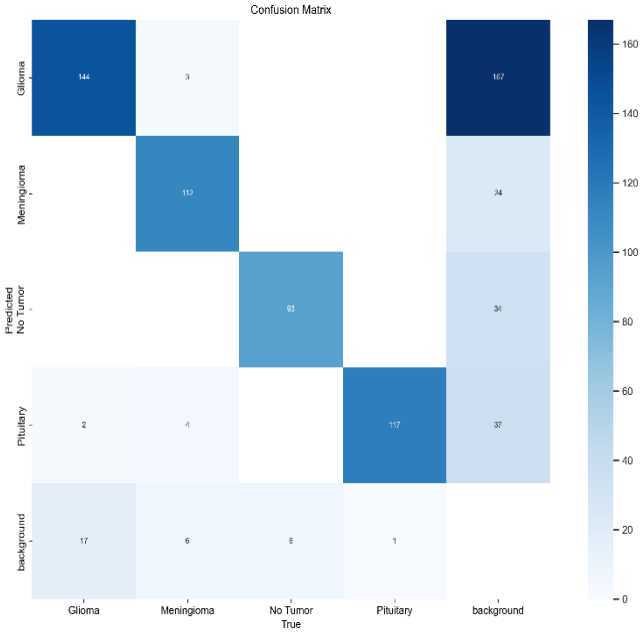

Figure 5: *Confusion Matrix*

C. *Performance Matrix*

Figure 6 presents the model's performance across training epochs:

Training and validation losses (bounding box, classification, and DFL) consistently decreased, confirming effective model convergence.

Both Precision and Recall improved steadily, reaching around 86% and 84%, respectively, by the final epoch.

mAP@0.5 and mAP@0.5:0.95 increased throughout training, with final values suggesting strong localization and classification accuracy.

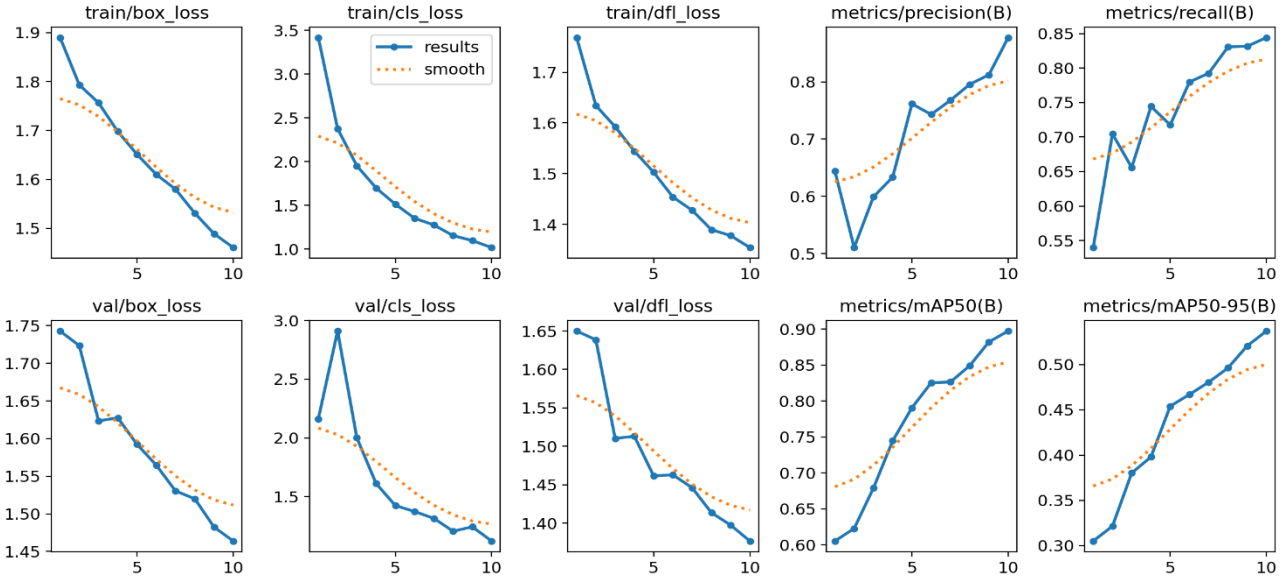

Figure 6: *Training and Testing Analysis*

epoch	time	train/box_loss	train/cls_loss	train/dfl_loss	metrics/precision(B)	metrics/recall(B)	metrics/mAP50(B)	metrics/mAP50-95(B)	val/box_loss	val/cls_loss	val/dfl_loss	lr/pg0	lr/pg1	lr/pg2
1	128.545	1.89007	3.41896	1.76839	0.6439	0.53974	0.60532	0.30496	1.74285	2.16249	1.64997	0.00041618	0.000416175	0.00041618
2	238.765	1.79328	2.37764	1.63434	0.51053	0.70455	0.62288	0.32148	1.72342	2.91116	1.63855	0.00075039	0.000750391	0.00075039
3	345.608	1.75657	1.95323	1.59263	0.59914	0.65585	0.6789	0.38019	1.62348	2.00094	1.51031	0.00100211	0.00100211	0.00100211
4	452.394	1.69787	1.70007	1.5444	0.6335	0.74444	0.74458	0.39782	1.62753	1.61165	1.51313	0.00087875	0.00087875	0.00087875
5	558.832	1.65106	1.51432	1.50299	0.76154	0.71763	0.79058	0.45391	1.59223	1.42382	1.46163	0.000755	0.000755	0.000755
6	675.802	1.60998	1.35347	1.45414	0.74305	0.78	0.8253	0.46685	1.56458	1.37297	1.46295	0.00063125	0.00063125	0.00063125
7	791.015	1.57983	1.27725	1.42796	0.76777	0.79256	0.8263	0.48044	1.53036	1.31472	1.44613	0.0005075	0.0005075	0.0005075
8	894.192	1.53096	1.15522	1.38978	0.79561	0.83076	0.849	0.49614	1.52001	1.20479	1.41377	0.00038375	0.00038375	0.00038375
9	998.77	1.48881	1.09853	1.37812	0.81234	0.83169	0.88204	0.52053	1.48236	1.24271	1.39761	0.00026	0.00026	0.00026
10	1104.19	1.46056	1.01855	1.35451	0.87737	0.84432	0.89719	0.53692	1.46383	1.12122	1.37687	0.00013625	0.00013625	0.00013625

Table 1: *Training and Testing Analysis*

V. CONCLUSION

The efficacy of the YOLO-based brain tumor detection and classification model in correctly identifying tumors in MRI scans has been demonstrated by its strong performance across all important metrics. The model's capacity to learn and optimize was validated by the consistent decrease in training and validation losses, such as box loss, classification loss, and distribution focal loss, over the epochs. The precision increased from 52.3% to 88.1%, demonstrating a significant improvement in the model's capacity to accurately identify pertinent tumor regions. Likewise, recall increased from 53.2% to 84.6%, demonstrating its enhanced ability to identify the majority of real tumor cases. With mAP@0.5 rising from 60.1% to 89.1% and mAP@0.5:0.95 reaching 54.1%, the mean Average Precision (mAP) also made significant strides, indicating the model's resilience even when evaluated against stringent criteria. Together, these findings support the suggested system's suitability, accuracy, and dependability for real-time medical image analysis, providing a potentially useful tool to support brain tumor early diagnosis and treatment planning.

REFERENCES

[1] Mohsen, Saeed, et al. "Brain Tumor Classification Using Hybrid Single Image Super-Resolution Technique with ResNext101_32x8d and VGG19 Pre-Trained Models." IEEE Access (2023).

[2] Solanki, Shubhangi, et al. "Brain Tumor Detection and Classification using Intelligence Techniques: An Overview." IEEE Access (2023).

[3] Shah, S. Muhammad Ahmed Hassan, et al. "Classifying and Localizing Abnormalities in Brain MRI using Channel Attention Based Semi-Bayesian Ensemble Voting Mechanism and Convolutional Auto-Encoder." IEEE Access (2023).

[4] Ferdous, Gazi Jannatul, et al. "LCDEiT: A Linear Complexity Data-Efficient Image Transformer for MRI Brain Tumor Classification." IEEE Access 11 (2023): 20337-20350.

[5] Ramprasad, M. V. S., Md Zia Ur Rahman, and Masreshaw D. Bayleyegn. "SBTC-Net: Secured Brain Tumor Segmentation and Classification Using Black Widow with Genetic Optimization in IoMT." IEEE Access (2023).

[6] Mohammed, Yahya MA, Said El Garouani, and Ismail Jellouli. "A survey of methods for brain tumor segmentation-based MRI images." Journal of Computational Design and Engineering 10.1 (2023): 266-293.

[7] Kazerooni, Anahita Fathi, et al. "The Brain Tumor Segmentation (BraTS) Challenge 2023: Focus on Pediatrics (CBTN-CONNECT-DIPGR-ASNR-MICCAI BraTS-PEDs)." ArXiv (2023).

[8] Chang, Yankang, et al. "Dpafnet: A residual dual-path attention-fusion convolutional neural network for multimodal brain tumor segmentation." Biomedical Signal Processing and Control 79 (2023): 104037.

[9] Moawad, Ahmed W., et al. "The Brain Tumor Segmentation (BraTS-METS) Challenge 2023: Brain Metastasis Segmentation on Pre-treatment MRI." ArXiv (2023).

[10] Peng, Yanjun, and Jindong Sun. "The multimodal MRI brain tumor segmentation based on AD-Net." Biomedical Signal Processing and Control 80 (2023): 104336.

[11] Madhan, S., & Kalaiselvan, A. (2024). Omics data classification using constitutive artificial neural network optimized with single candidate optimizer. Network: Computation in Neural Systems, 1–25.